Superconductivity and Correlated Insulator in Twisted Bilayer Graphene

Liang Fu

with Noah Yuan and Hiroki Isobe

University of Minnesota, 05/18/2018

Outline

- Effective TB model: honeycomb lattice, (p_x,p_y)-orbital

  Noah Yuan & LF, arXiv: 1803.09699

  TB model with specific hopping parameters:

  Koshino, Yuan, Ochi, Kuroki & LF, arXiv: 1805.06819

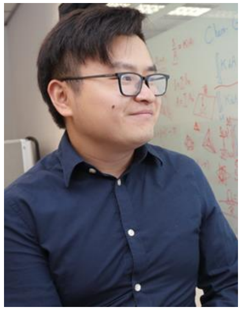

- Electronic instabilities from weak-coupling

  Hiroki Isobe, Yuan & LF, arXiv: 1805.06449

Nearly-Flat Band at Magic Angle

Bistritzer & MacDonald, PNAS (2011)

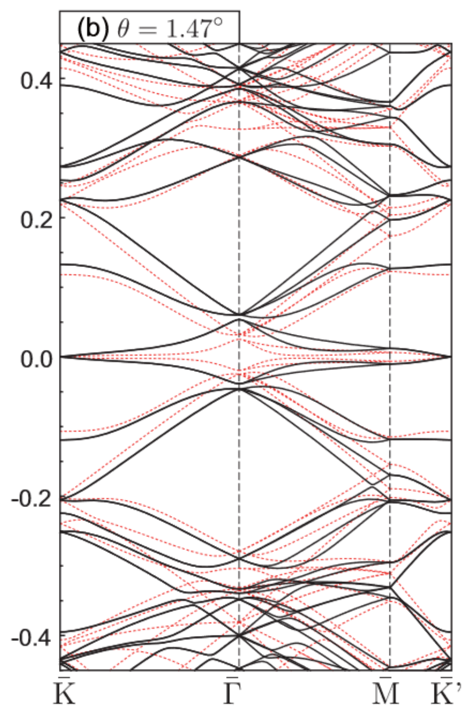

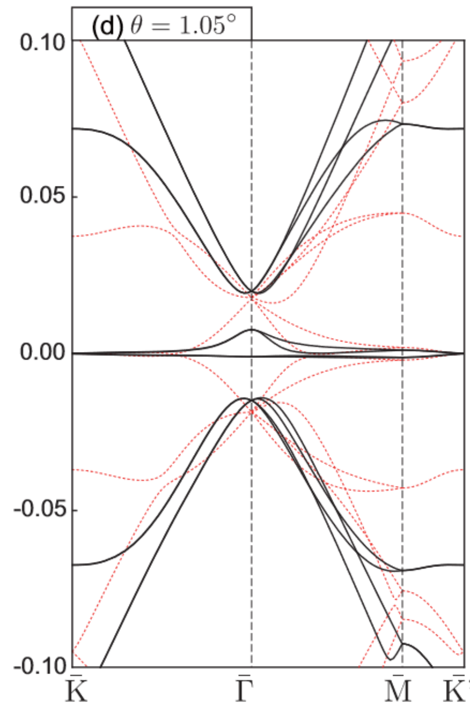

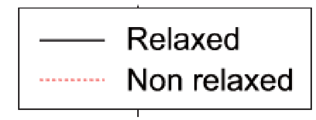

Lam & Koshino PRB (2017)

- Gap at **Γ** point separates 4 lowest-energy mini-bands from others
- Inter-valley hybridization can be neglected at small twist angle:

  => 2 mini-band from vicinity of K; 2 from -K
- at magic angle, mini-band width of order 10meV

Our Approach

to construct TB model for isolated lowest-energy band

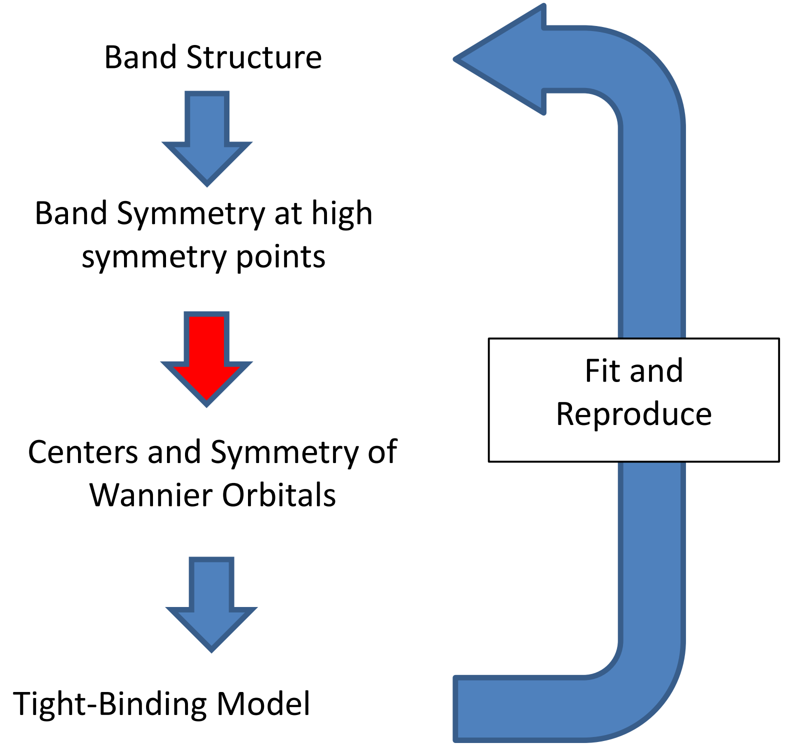

Noah Yuan & LF, arXiv: 1803.09699

Our Approach

to construct TB model for isolated lowest-energy band

Q: what kind of Wannier orbital configuration in real space can reproduce band symmetry in k space?

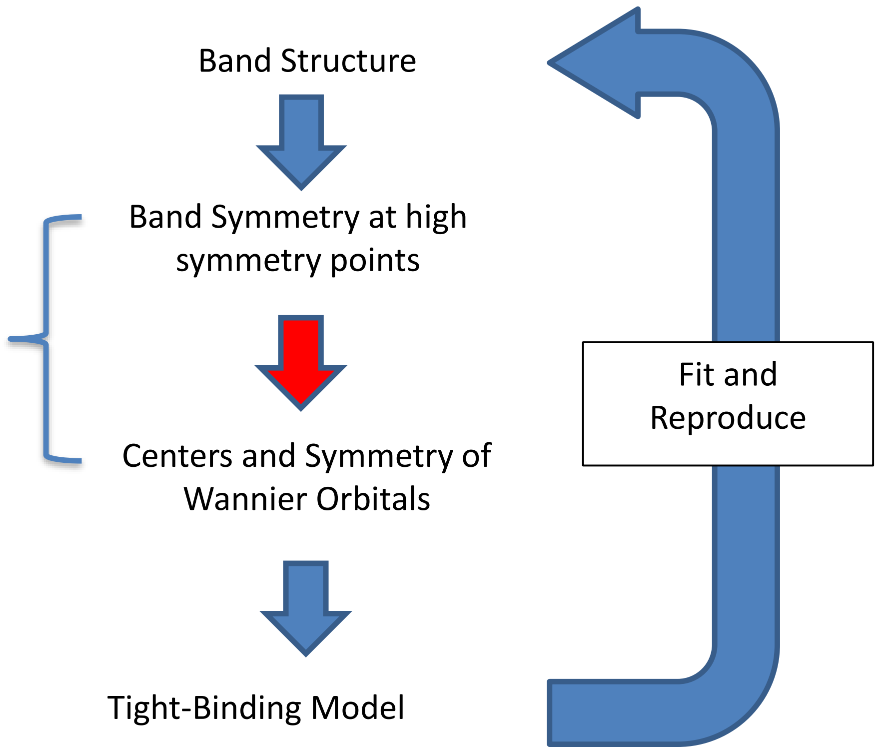

Noah Yuan & LF, arXiv: 1803.09699

Note: Wannier orbitals associated with a set of bands do not depend on $E_i(k)$

Coordinate System in Real Space

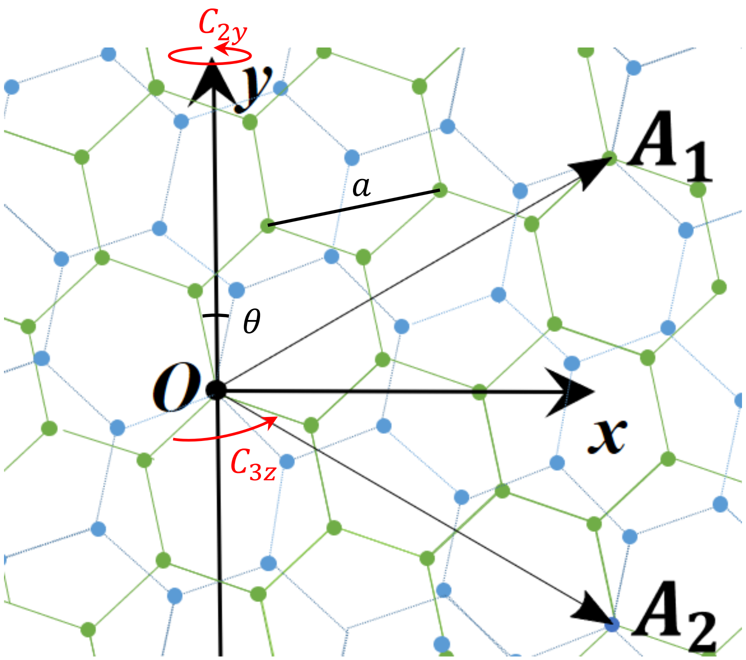

In this figure $\theta = 21.8^{\circ}$ for illustration

Generators of point group D_3:

Three-fold rotation C_{3z} around **registered** A sites, denoted as the origin O;

Two-fold rotation C_{2y} around y axis passing through the origin.

Symmetry Group Representation

Point group $D_3 = \{C_{3z}^m, C_{2y}^n | m, n \in \mathbb{Z}\}$

1D Reps A_1: $C_{3z} = C_{2y} = +1,$ s-orbital

A_2: $C_{3z} = +1, C_{2y} = -1.$ p_z-orbital

2D Rep E: $C_{3z} = \begin{pmatrix} e^{-2i\pi/3} & 0 \\ 0 & e^{2i\pi/3} \end{pmatrix}, \ C_{2y} = \begin{pmatrix} 0 & 1 \\ 1 & 0 \end{pmatrix}$

p_x, p_y-orbital

Coordinate System in k-Space

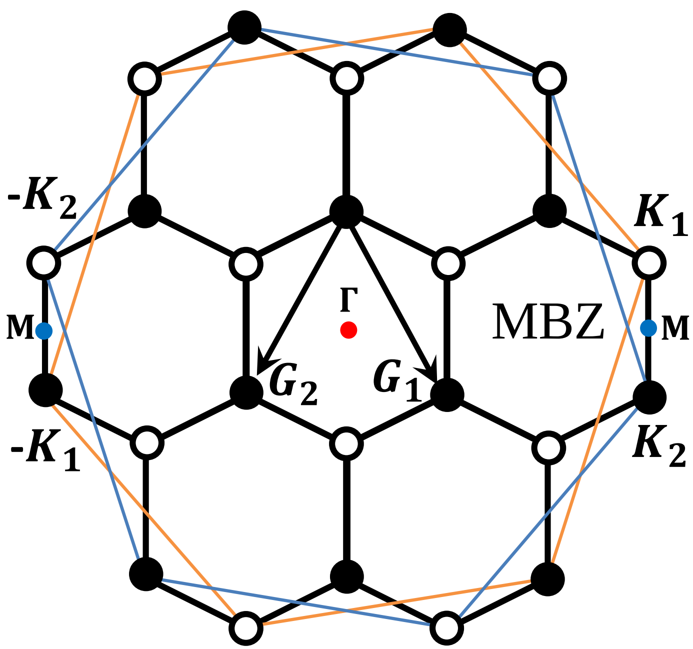

Valley folding:

$$\boldsymbol{K}_1, -\boldsymbol{K}_2 \rightarrow +\boldsymbol{K}$$
$$\boldsymbol{K}_2, -\boldsymbol{K}_1 \rightarrow -\boldsymbol{K}$$

Example: Monolayer Graphene

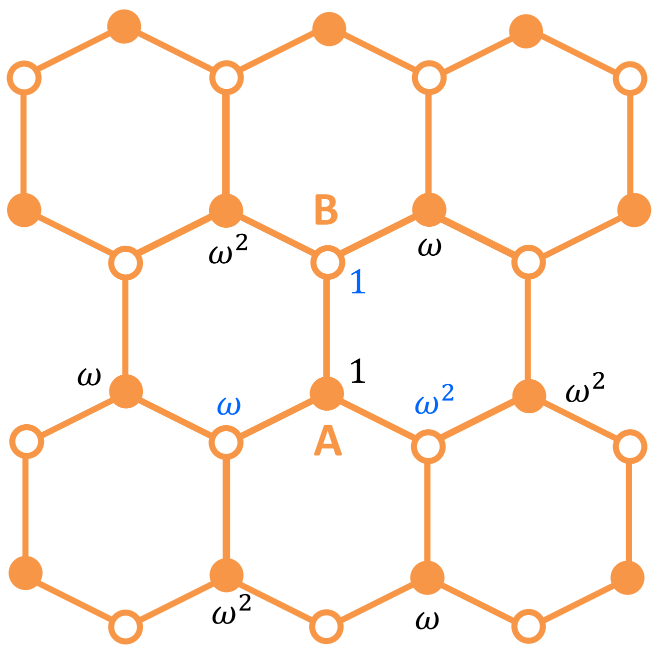

$$\omega = e^{2i\pi/3} = \exp(iK \cdot R)$$

At +/-***K*** point, the Bloch wave functions of A, B sites will assign different phases to different sites.

With respect to rotation center of C_{3z} at A site, Bloch states at A sites have $L_z = 0$.

Bloch states at B sites have $L_z = 1$ at +K and $L_z = -1$ at -K

Band Symmetry at $\boldsymbol{K}$ Point

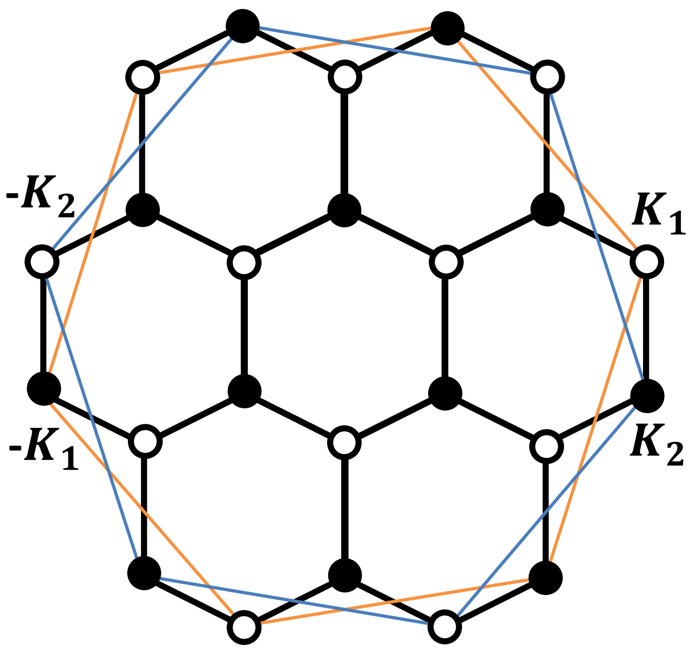

A_1: $\xi_+^A + \eta_-^A$ A_2: $\xi_+^A - \eta_-^A$

E: (ξ_+^B, η_-^B)

$\boldsymbol{K}$ point: Symmetry group D_3

$$\boldsymbol{K}_1, -\boldsymbol{K}_2 \rightarrow +\boldsymbol{K}$$
$$\boldsymbol{K}_2, -\boldsymbol{K}_1 \rightarrow -\boldsymbol{K}$$

From valley folding scheme, the lowest four bands form two singlets and one doublet.

$$(A_1, A_2, E)$$

(Four degenerate states at Dirac point are NOT exact, and NOT protected by any lattice symmetry.)

Band Symmetry at $\boldsymbol{M}$ Point

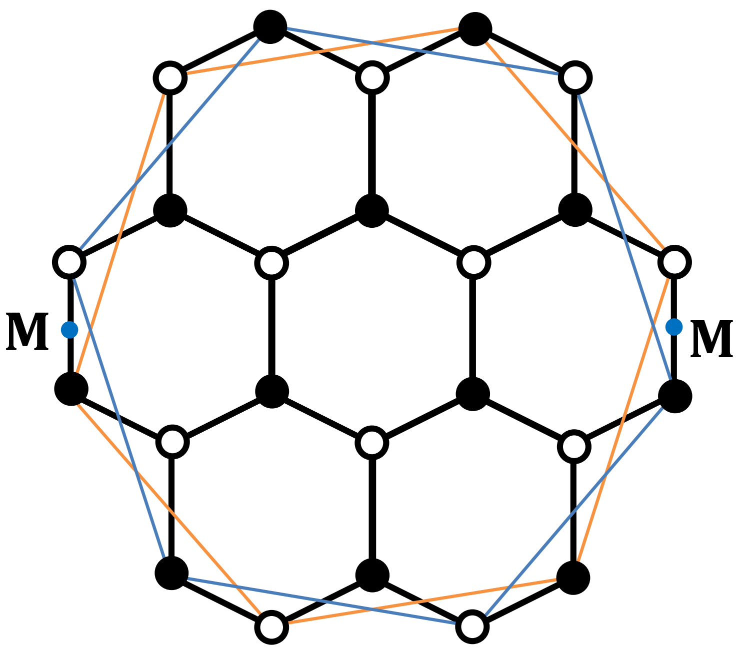

A: $\xi^n_{+M} + \eta^n_{-M}$ B: $\xi^n_{+M} - \eta^n_{-M}$

n=A, B is sublattice index.

$\boldsymbol{M}$ point: Symmetry group C_2

From valley folding scheme, the lowest four bands form four singlets.

$$(A, A, B, B)$$

Band Symmetry at $\boldsymbol{\Gamma}$

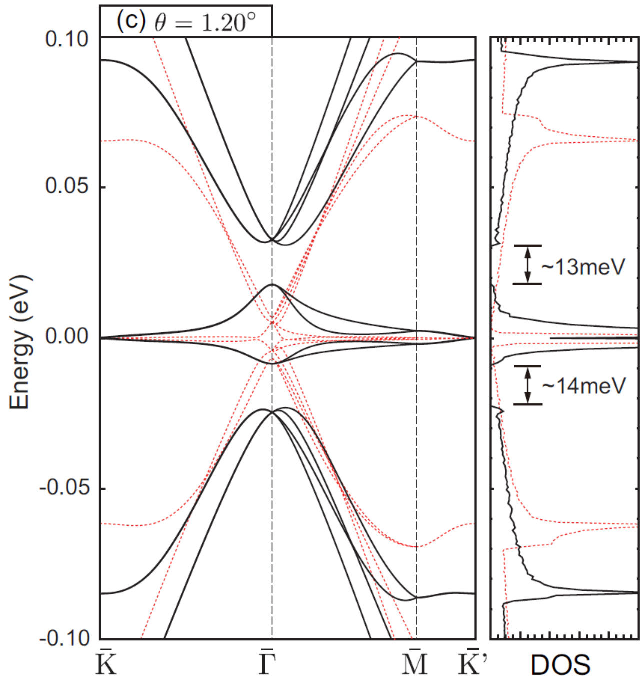

Nguyen N. T. Nam and Mikito Koshino, PRB **96**, 075311 (2017).

$\boldsymbol{\Gamma}$ point: Symmetry group D_3

We infer the lowest four bands furnish two doublets on electron and hole sides.

$$(E, E)$$

Band Symmetry at High Symmetry Points

	Γ	K	M
Group	D_3	D_3	C_2
Reps	$\{E, E\}$	$\{A_1, A_2, E\}$	$\{A, A, B, B\}$
C_{3z}	$\{\pm 1, \pm 1\}$	$\{0, 0, \pm 1\}$	NA
C_{2y}	NA	$\{+1, -1, \mathrm{NA}\}$	$\{+1, +1, -1, -1\}$

Q: what kind of Wannier orbital configuration in real space can reproduce the above band symmetry in k space?

Centers & Symmetries of Wannier Orbitals

Noah Yuan & LF, arXiv: 1803.09699

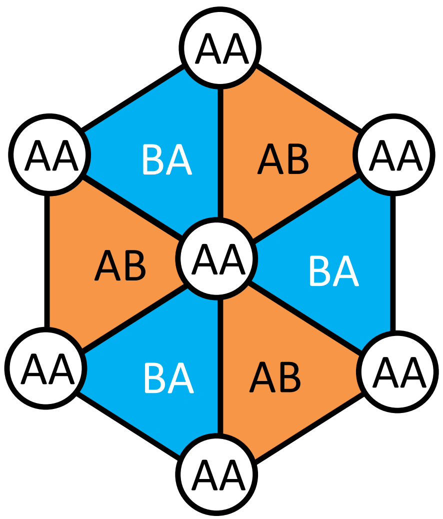

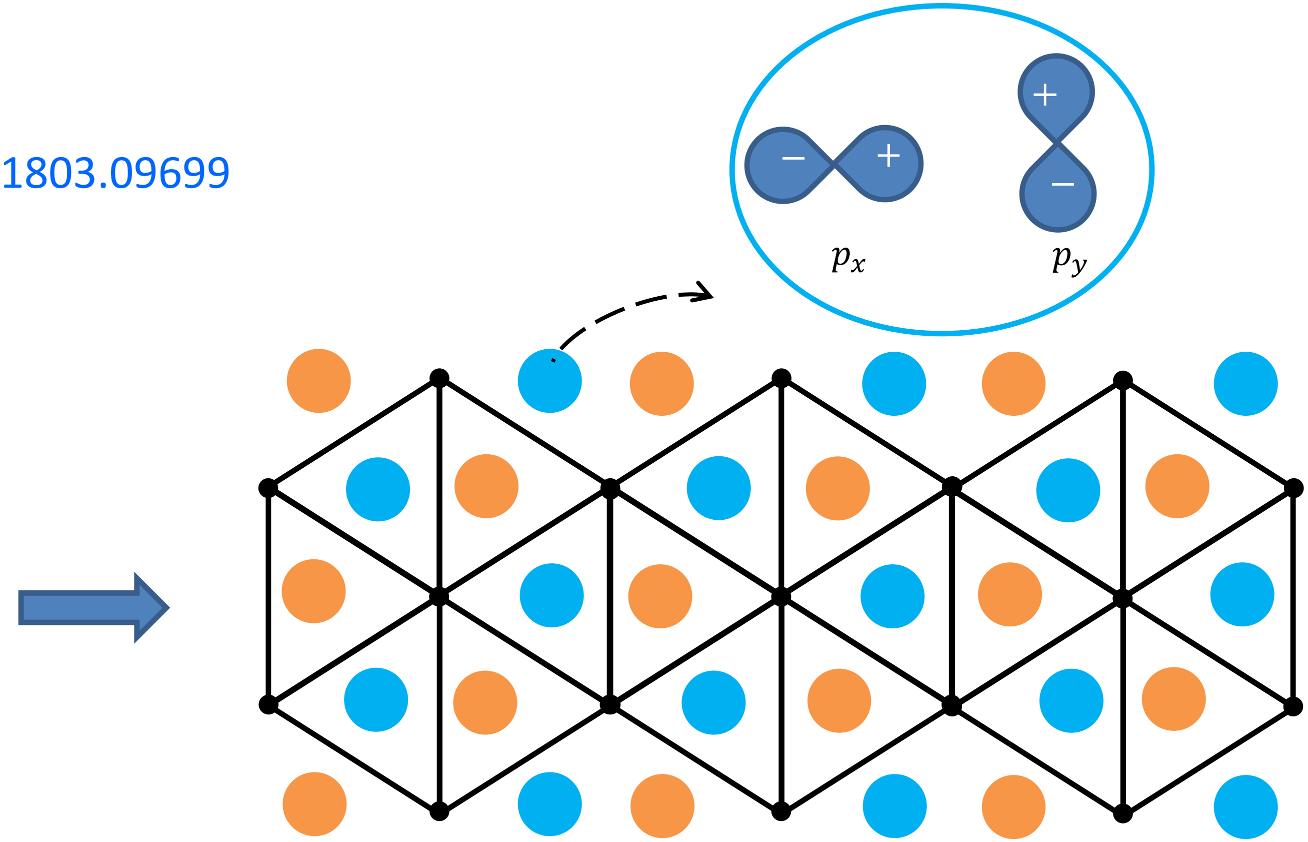

- Wannier centers are located at C_{3z}-symmetric AB and BA points, and form a honeycomb superlattice.
- A doublet of Wannier orbitals at each honeycomb site, with (p_x,p_y) site symmetry

Band Symmetry at High Symmetry Points

	Γ	K	M
Group	D_3	D_3	C_2
Reps	$\{E, E\}$	$\{A_1, A_2, E\}$	$\{A, A, B, B\}$
C_{3z}	$\{\pm1, \pm1\}$	$\{0, 0, \pm1\}$	NA
C_{2y}	NA	$\{+1, -1, \text{NA}\}$	$\{+1, +1, -1, -1\}$

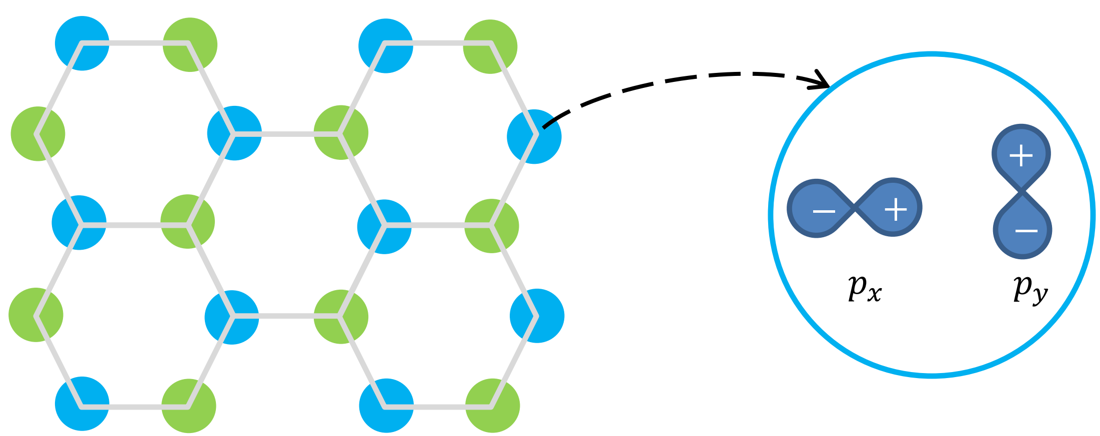

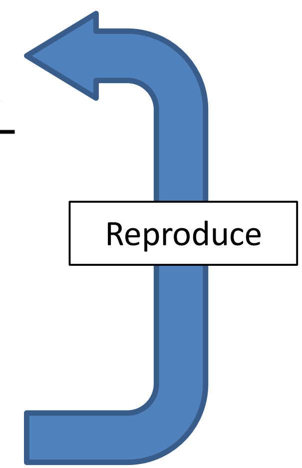

Tight-Binding Model: hexagonal warping

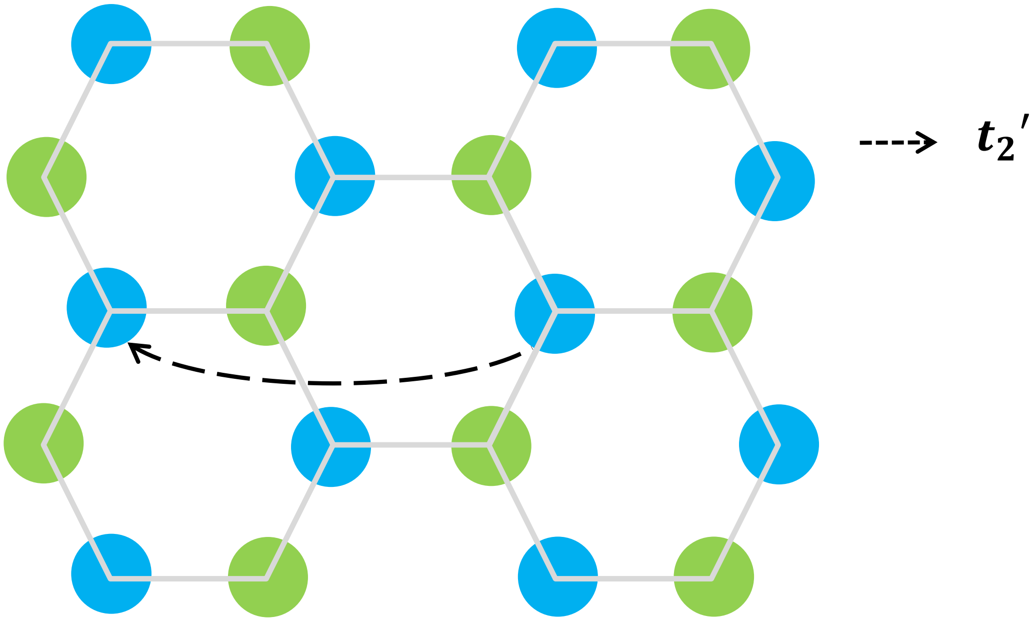

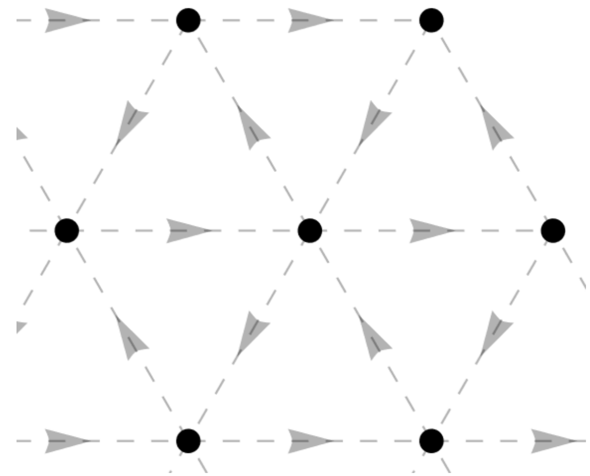

$$H_{\text{hex}} = t_2' \sum_{ij} (\mathbf{c}_i^\dagger \times \mathbf{c}_j)_z + h.c. \qquad \mathbf{c} = (c_x, c_y)$$

Equivalent to second nearest neighbors within the same sublattice with imaginary amplitudes according to the arrows, opposite for two valleys

Hexagonal warping

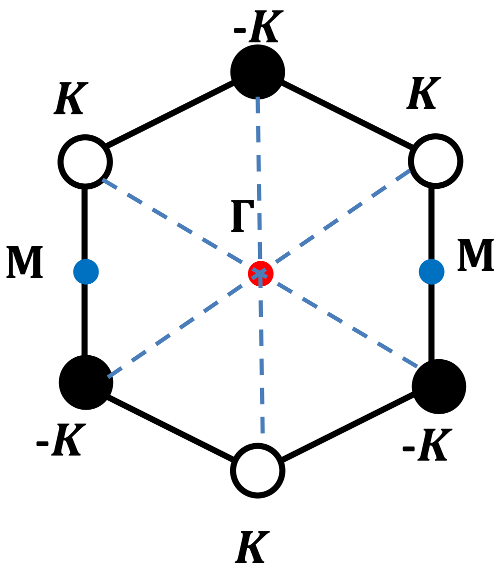

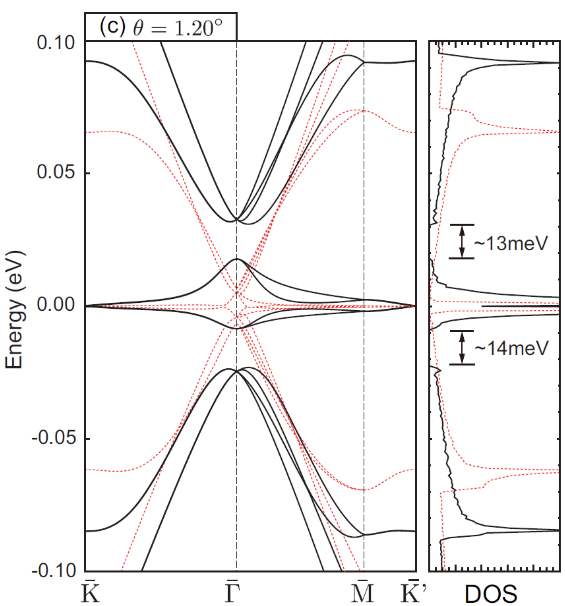

Nodal line of hexagonal warping term

Near **Γ** point

$$H_{\text{hex}}(\boldsymbol{k}) = -\frac{3\sqrt{3}A^3 t_2'}{16}(k_+^3 + k_-^3)\tau_z$$

$$(c_+, c_-)^{\mathrm{T}} \text{ where } c_\pm = (c_x \pm i c_y)/\sqrt{2}$$

$$k_\pm = k_x \pm i k_y$$

Selected for a Viewpoint in *Physics*
PRL **103**, 266801 (2009) PHYSICAL REVIEW LETTERS week ending 31 DECEMBER 2009

Hexagonal Warping Effects in the Surface States of the Topological Insulator Bi_2Te_3

Liang Fu*

$$H(\vec{k}) = E_0(k) + v_k(k_x\sigma_y - k_y\sigma_x) + \frac{\lambda}{2}(k_+^3 + k_-^3)\sigma_z,$$

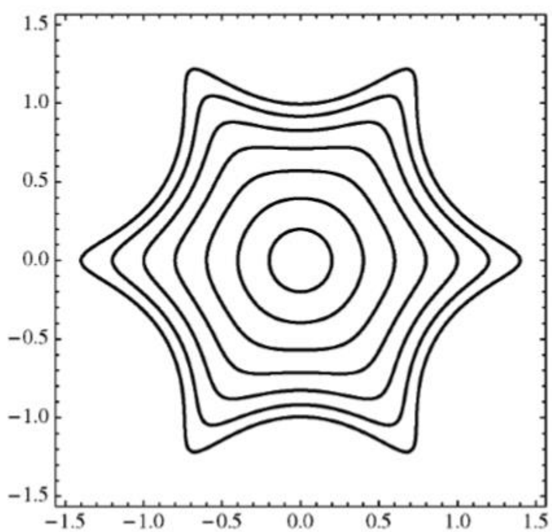

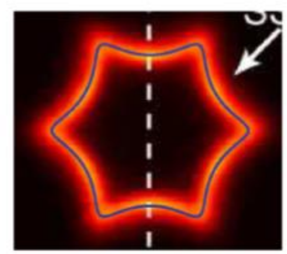

Tight-Binding Model: Fitting

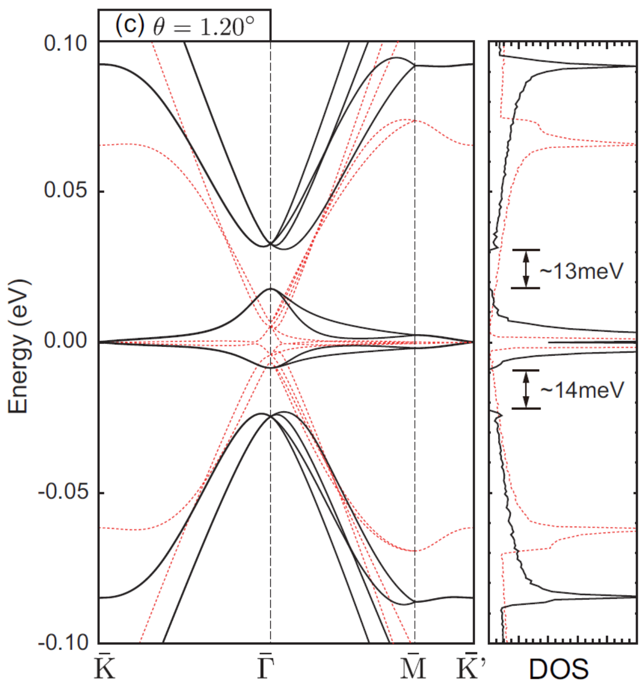

Nguyen N. T. Nam and Mikito Koshino, PRB **96**, 075311 (2017).

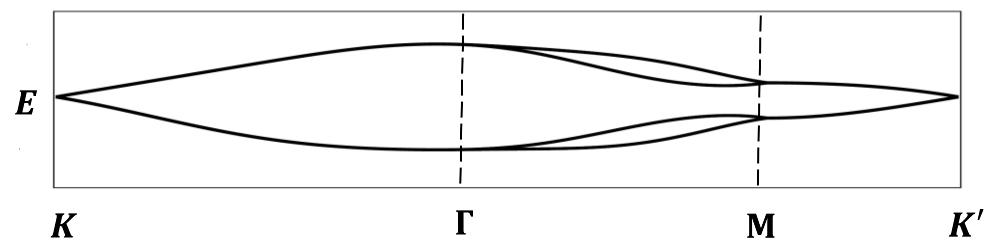

Maximally-localized Wannier orbitals and the extended Hubbard model for the twisted bilayer graphene

Mikito Koshino,[1,*] Noah F. Q. Yuan,[2] Masayuki Ochi,[1] Kazuhiko Kuroki,[1] and Liang Fu[2]

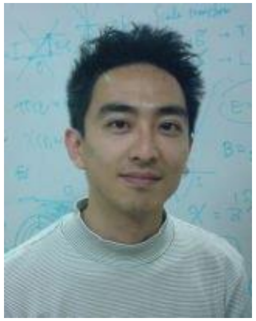

"The obtained Wannier state is centered at AB or BA point… the pair of Wannier orbitals centered at a given AB or BA point has px,py on-site symmetry… consistent with the symmetry analysis [4]."

"According to the symmetry analysis [4], the two orbitals should be centered at AB and BA points to form a honeycomb lattice. Our strategy is to first prepare certain initial orbitals centered at AB and BA, and then apply the maximally localized algorithm [39]"

AB / BA-centered Wannier functions: p_x+ip_y symmetry

Orbital 1 (A-like): AB-centered

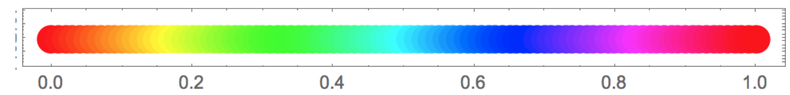

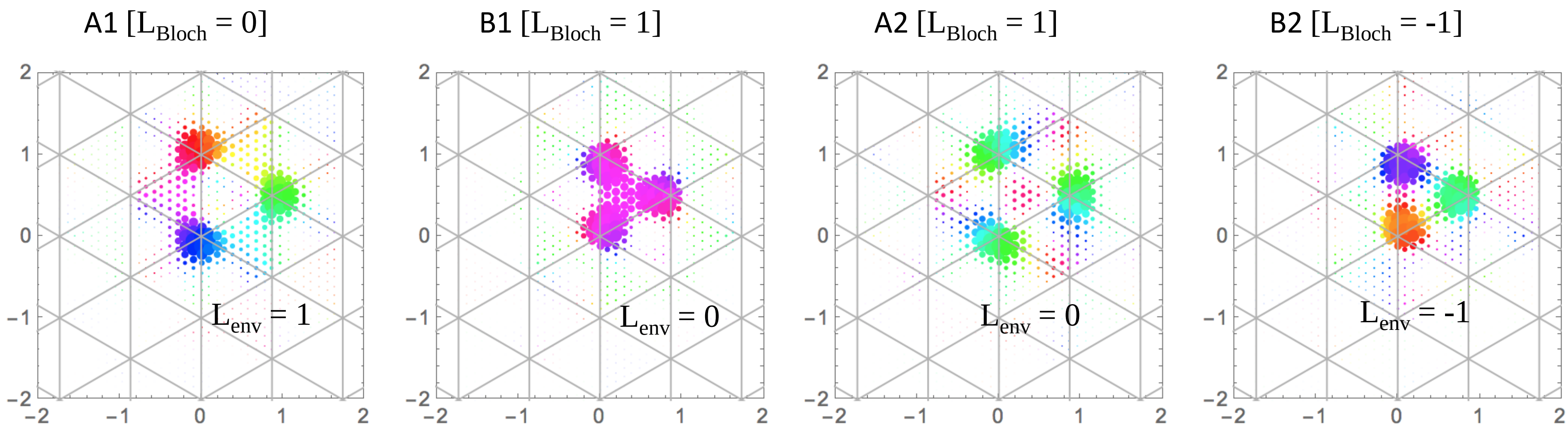

Orbital 2 (B-like) : BA-centered

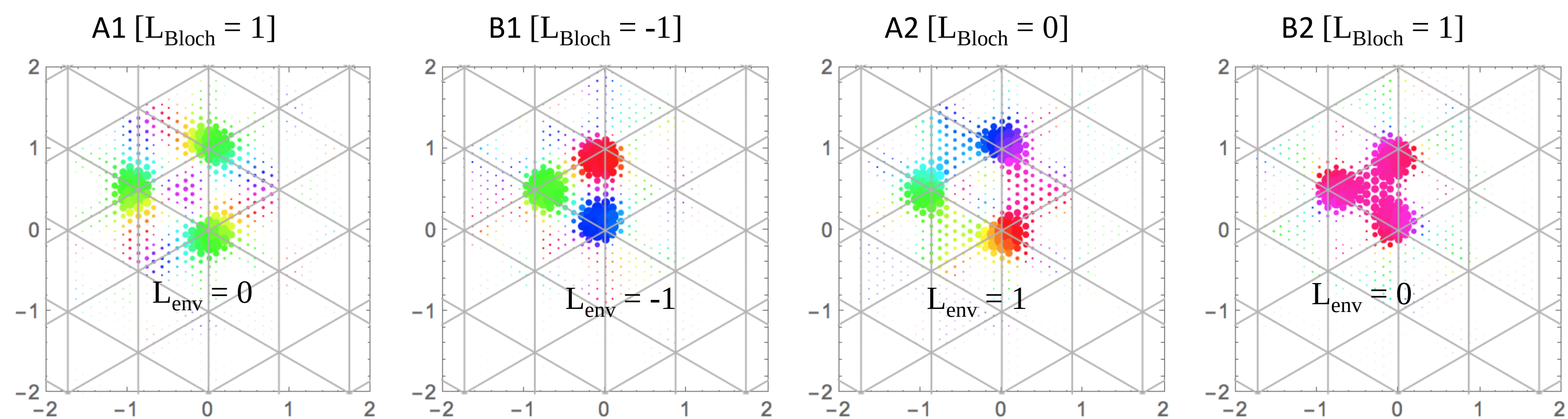

TB Model with Realistic Parameters

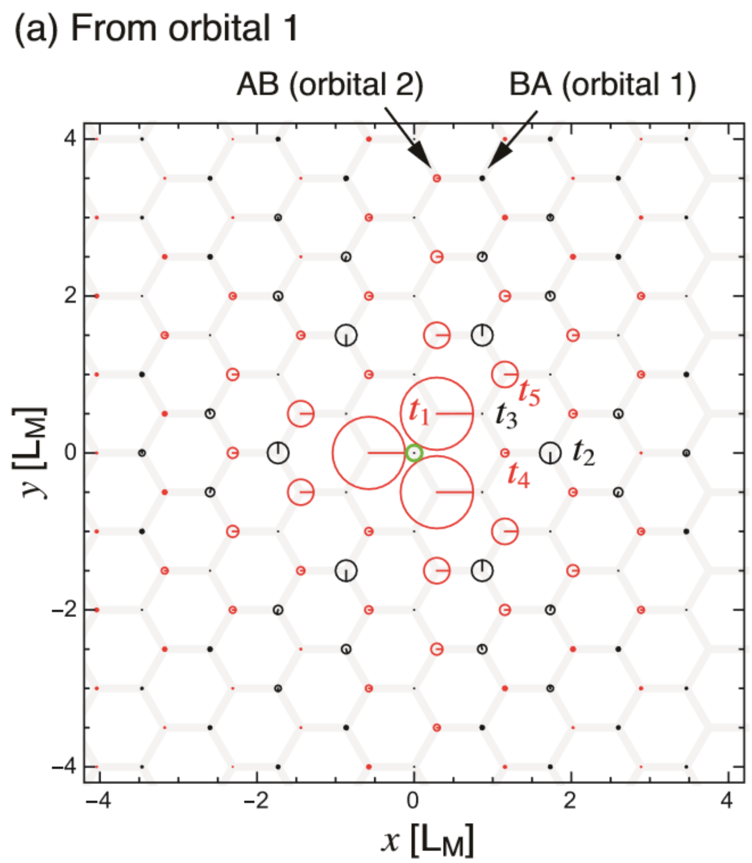

Three dominant hoppings: t_1, t_2 (imaginary), t_5

Superconductivity & Correlated Insulator at *ϑ=1.1*

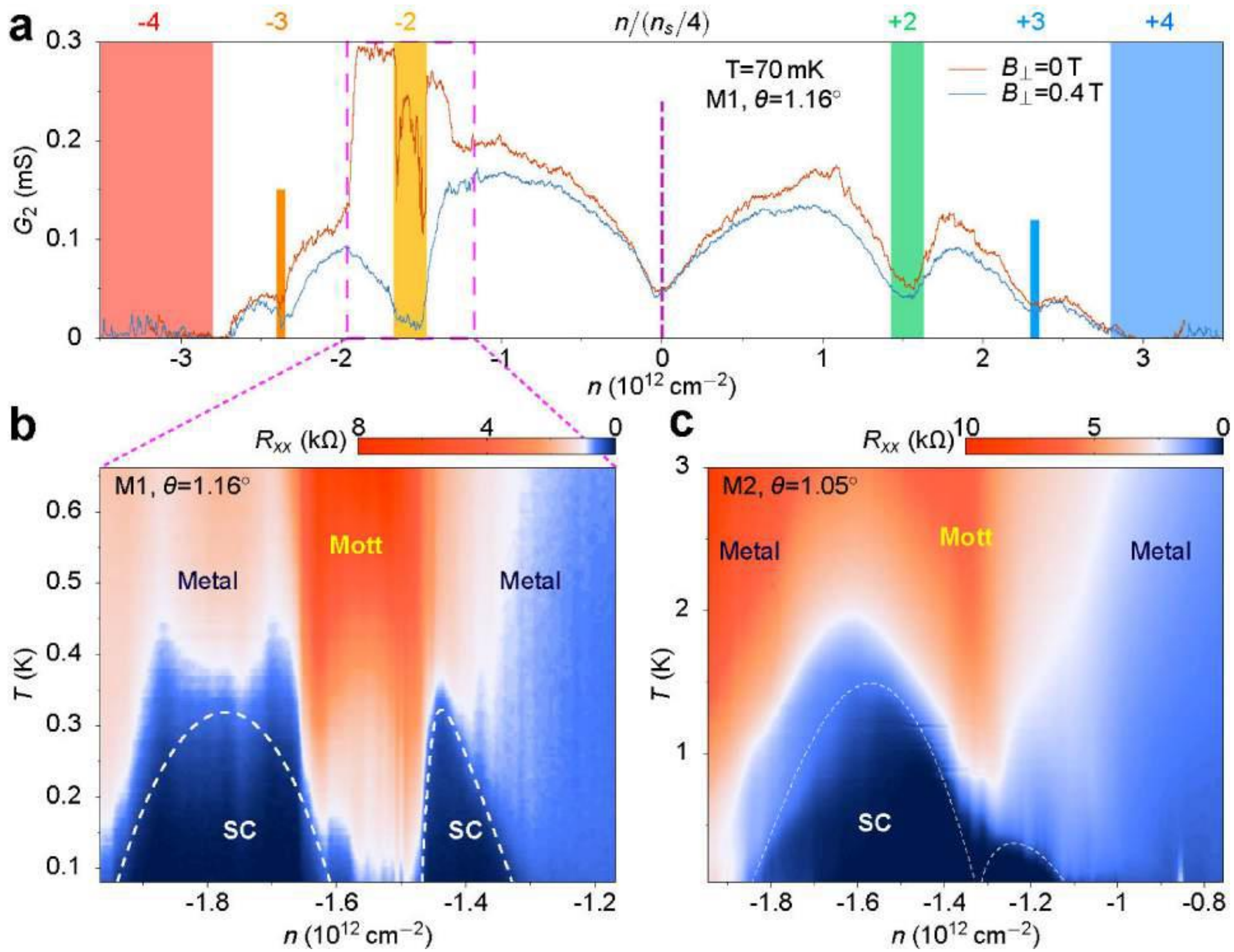

Normal State at ϑ=1.8

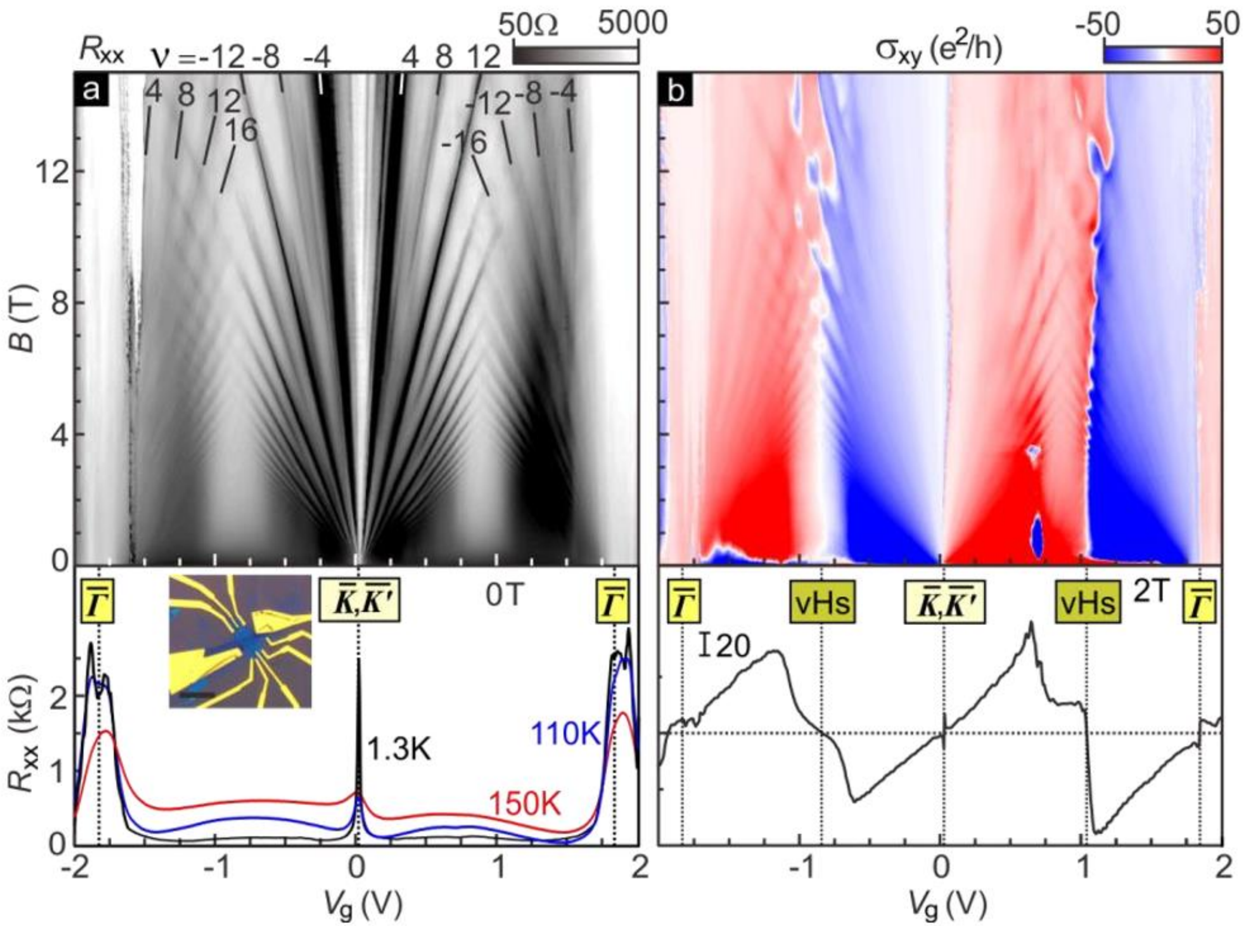

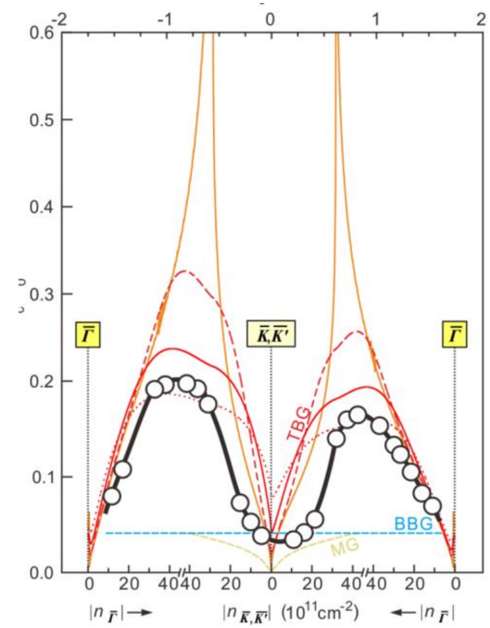

Kim et al, Nano Lett (2016)

Hall conductivity changes sign when Fermi surface changes from electron to hole-like

Fermi Surface, Lifshitz Transition & Van Hove Singularity

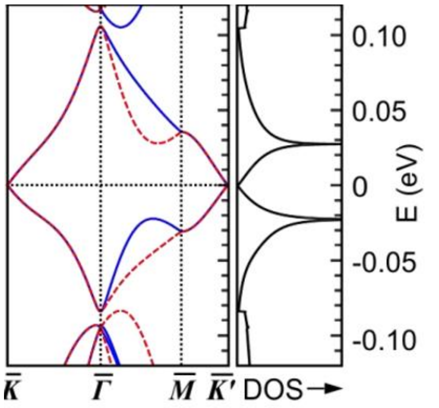

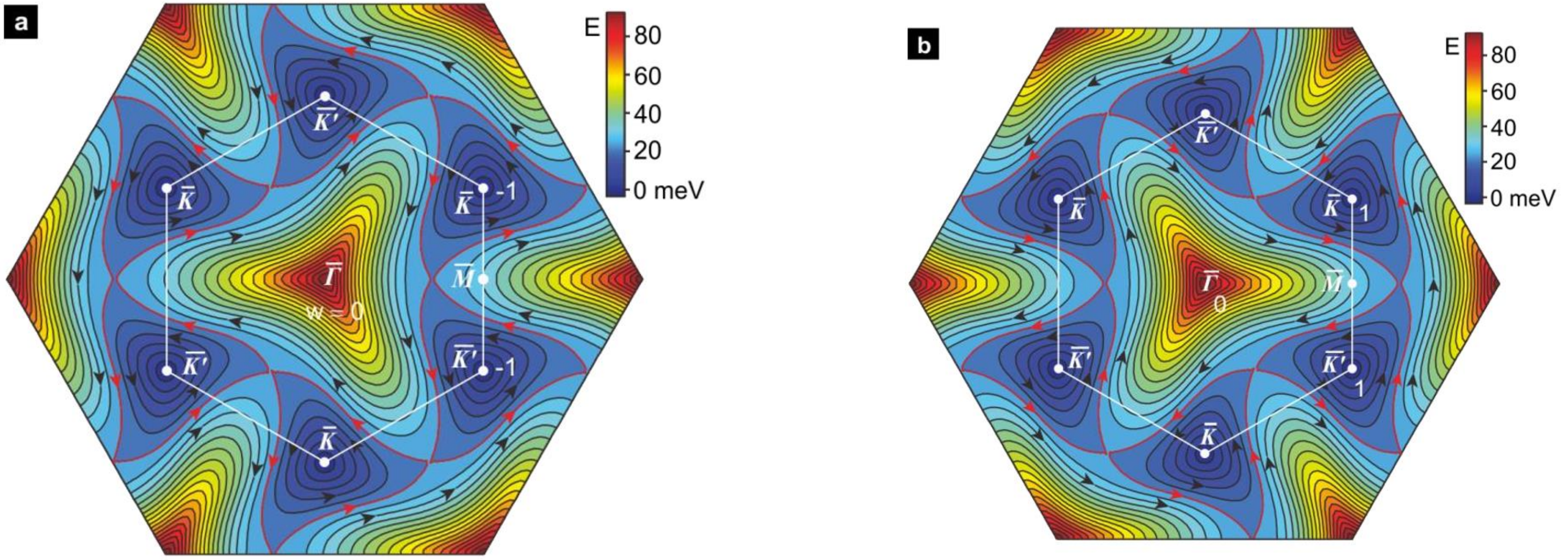

- Below VHS, electron pockets around Dirac point
- Above VHS, warped hole pockets around **Γ** point

Van Hove Singularity seen in STM

ϑ=1.8

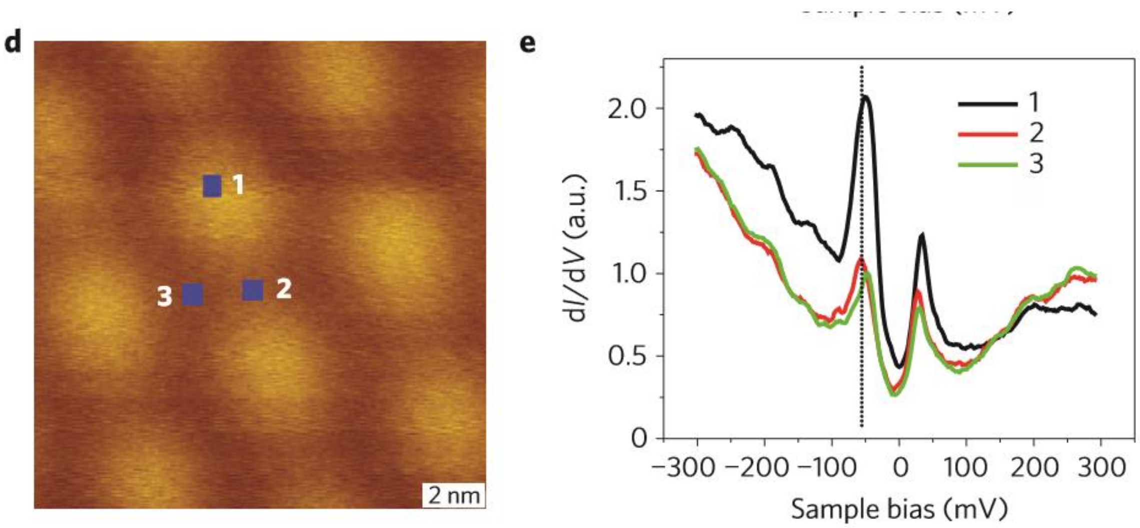

ϑ=1.1

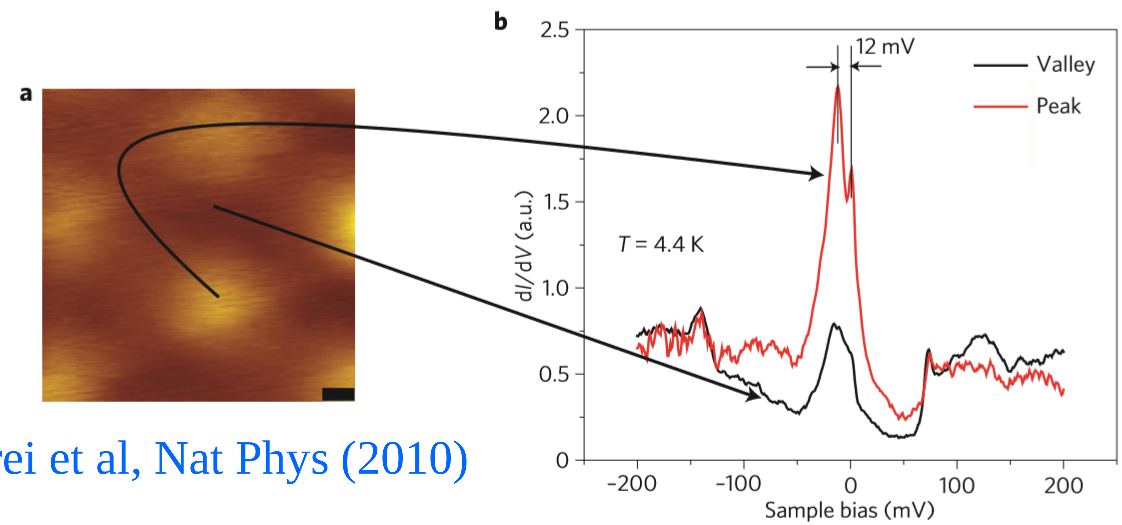

Eva Andrei et al, Nat Phys (2010)

Fermi Surface Nesting and Hot Spots

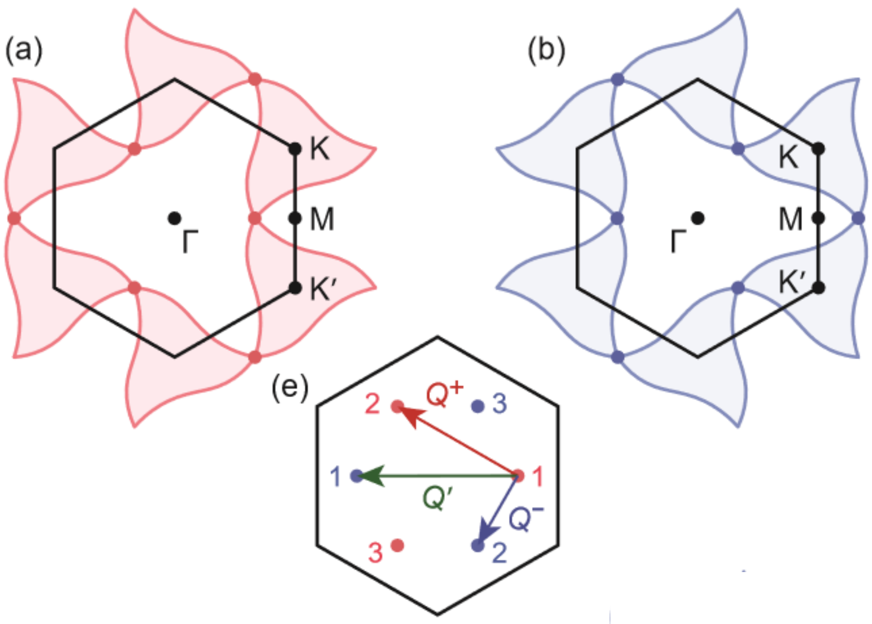

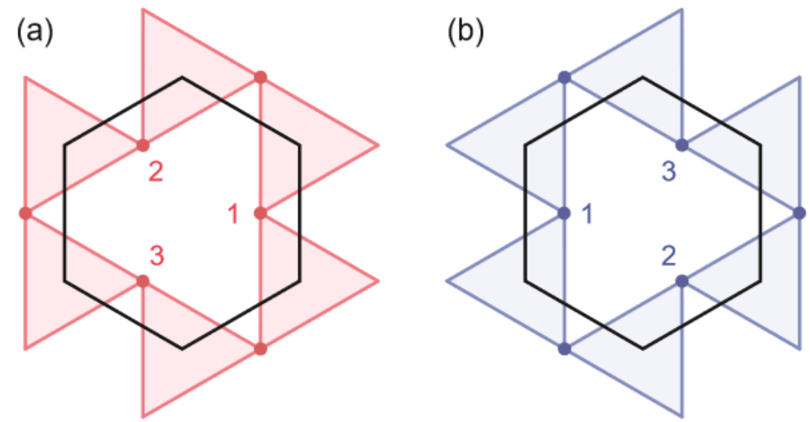

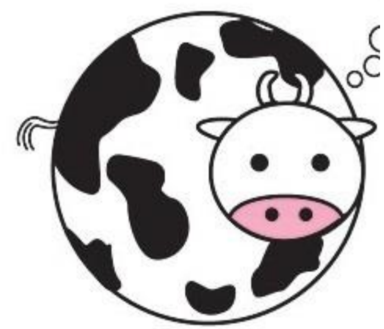

Fermi Surface Nesting and Hot Spots

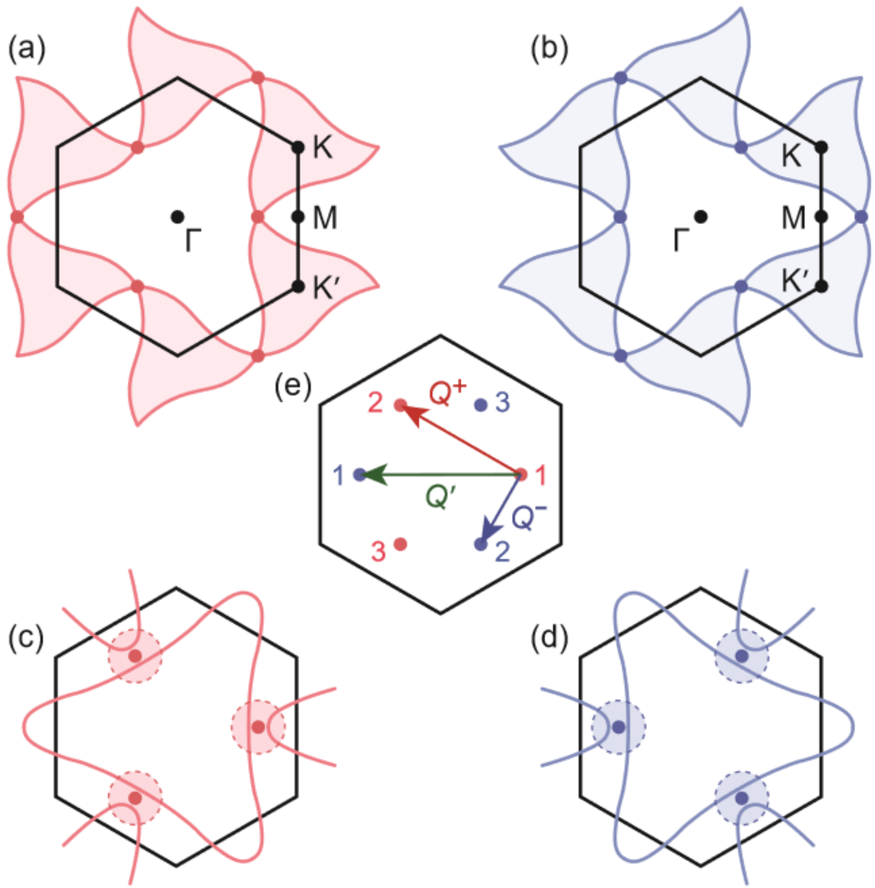

Three distinct wave vectors (Q+, Q−, Q’), along with symmetry-related ones, connect nearly nested segments of Fermi surfaces where density of states are large.

↓

Enhanced fluctuations of inter-valley density waves at Q’ and Q-, and pair density wave at Q+

Hot spot approach: poor man’s functional RG

Chiral superconductivity from repulsive interactions in doped graphene

Rahul Nandkishore[1], L. S. Levitov[1] and A. V. Chubukov[2]*

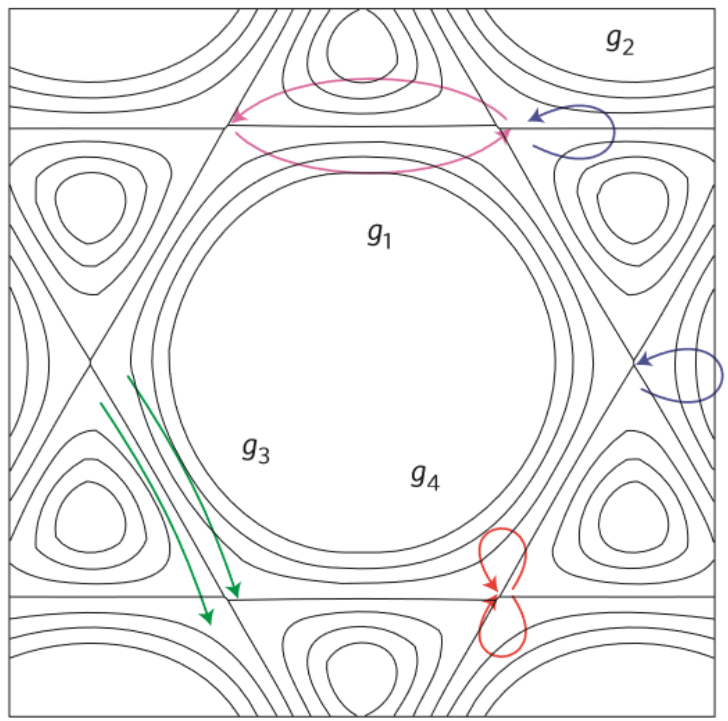

Scattering Processes

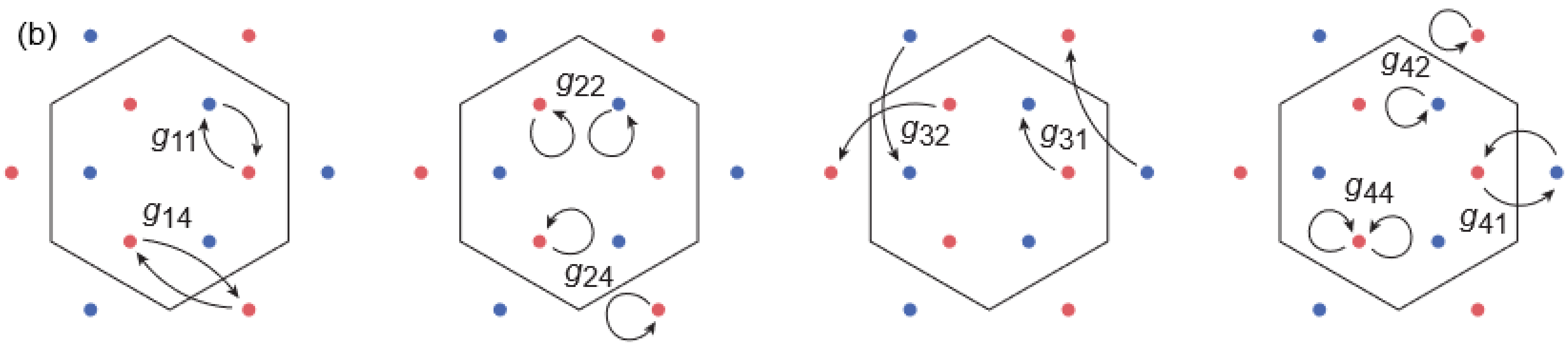

- g11, g14, g22, g24, g44: forward scattering processes
- g31, g32, g41, g42: BCS scattering processes

RG Equation for 9 Coupling Constants

$$
\begin{aligned}
\dot{g}_{11} =& - 2d_{3-}g_{11}g_{22} + 2d_{2+}(g_{11}g_{44} + g_{14}g_{41}) \\
& + 2d_{1-}(g_{11}g_{22} - g_{11}^2 + g_{31}g_{32} - g_{31}^2), \\
\dot{g}_{14} =& - 2d_{3+}g_{14}g_{24} + 2d_{2+}(g_{14}g_{44} + g_{11}g_{41}) \\
& + 2d_{1+}(g_{14}g_{24} - g_{14}^2 + g_{31}g_{32} - g_{32}^2), \\
\dot{g}_{22} =& - d_{3-}(g_{11}^2 + g_{22}^2) + d_{1-}(g_{22}^2 + g_{32}^2) \\
& + 2d_{2+}[(g_{11} - g_{22})g_{44} + g_{14}g_{42} + g_{24}(g_{41} - 2g_{42})], \\
\dot{g}_{24} =& - d_{3+}(g_{14}^2 + g_{24}^2) + d_{1+}(g_{24}^2 + g_{31}^2) \\
& + 2d_{2+}[(g_{11} - 2g_{22})g_{42} + (g_{14} - g_{24})g_{44} + g_{22}g_{41}], \\
\dot{g}_{31} =& - 2(g_{31}g_{32} + g_{31}g_{42} + g_{32}g_{41}) + 2d_{1+}g_{24}g_{31} \\
& + 2d_{1-}(g_{11}g_{32} + g_{22}g_{31} - 2g_{11}g_{31}), \\
\dot{g}_{32} =& - (g_{31}^2 + g_{32}^2 + 2g_{31}g_{41} + 2g_{32}g_{42}) \\
& + 2d_{1-}g_{22}g_{32} + 2d_{1+}(g_{14}g_{31} + g_{24}g_{32} - 2g_{14}g_{32}), \\
\dot{g}_{41} =& - 2(2g_{31}g_{32} + g_{41}g_{42}) \\
& + 2d_{2+}(2g_{11}g_{14} + g_{41}g_{44}) + 2d_{2-}(g_{41}g_{42} - g_{41}^2), \\
\dot{g}_{42} =& - (2g_{31}^2 + 2g_{32}^2 + g_{41}^2 + g_{42}^2) + d_{2-}g_{42}^2 \\
& + 2d_{2+}[2g_{11}g_{24} + 2g_{14}g_{22} + (g_{41} - g_{42})g_{44} - 4g_{22}g_{24}], \\
\dot{g}_{44} =& - d_{0+}g_{44}^2 + d_{2+}(2g_{11}^2 + 4g_{11}g_{22} + 2g_{14}^2 + 4g_{14}g_{24} \\
& - 4g_{22}^2 - 4g_{24}^2 + g_{41}^2 + 2g_{41}g_{42} - 2g_{42}^2 + g_{44}^2).
\end{aligned}
$$

RG Equation for 2 Coupling Constants

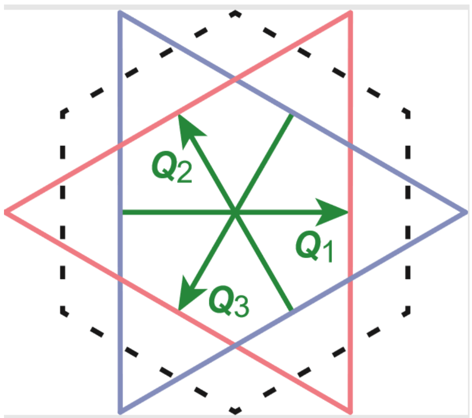

$$\dot{g}_{41} = -2g_{41}g_{42} + 2d_{2-}(g_{41}g_{42} - g_{41}^2),$$
$$\dot{g}_{42} = -(g_{41}^2 + g_{42}^2) + d_{2-}g_{42}^2.$$

- g_{42} : inter-valley density interaction
- g_{41} : valley exchange interaction

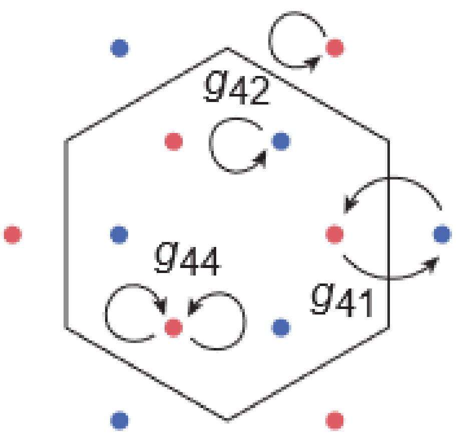

Parameter d characterizes density wave susceptibility.

d=1 corresponds to same log divergent as BCS channel

Here d<1 is approximately constant within the energy range where Fermi surface can be regarded as nested, i.e., susceptibility has logarithmic dependence on energy

Intertwined SC and Density Wave

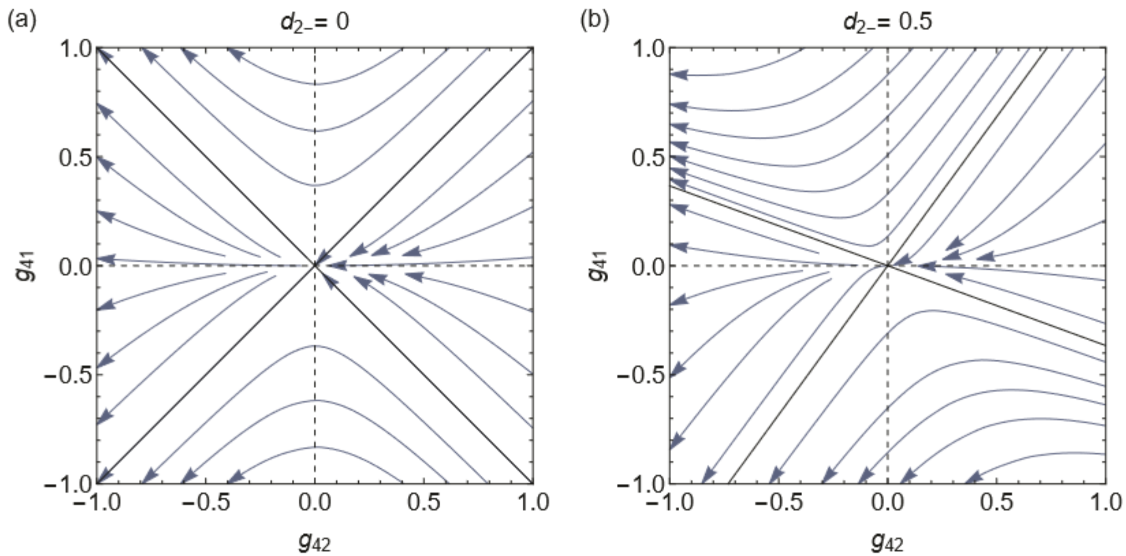

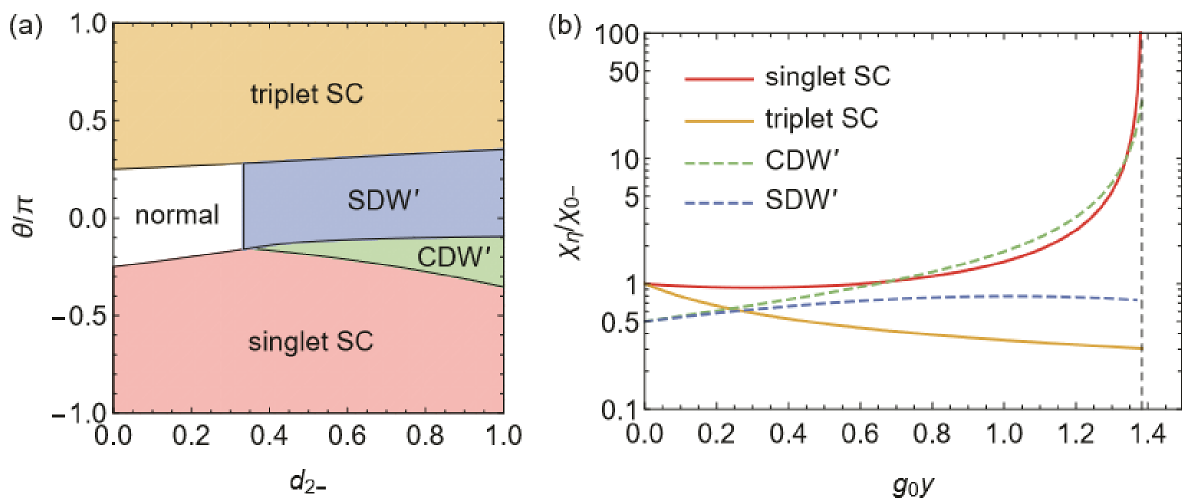

Comparison with Experiment

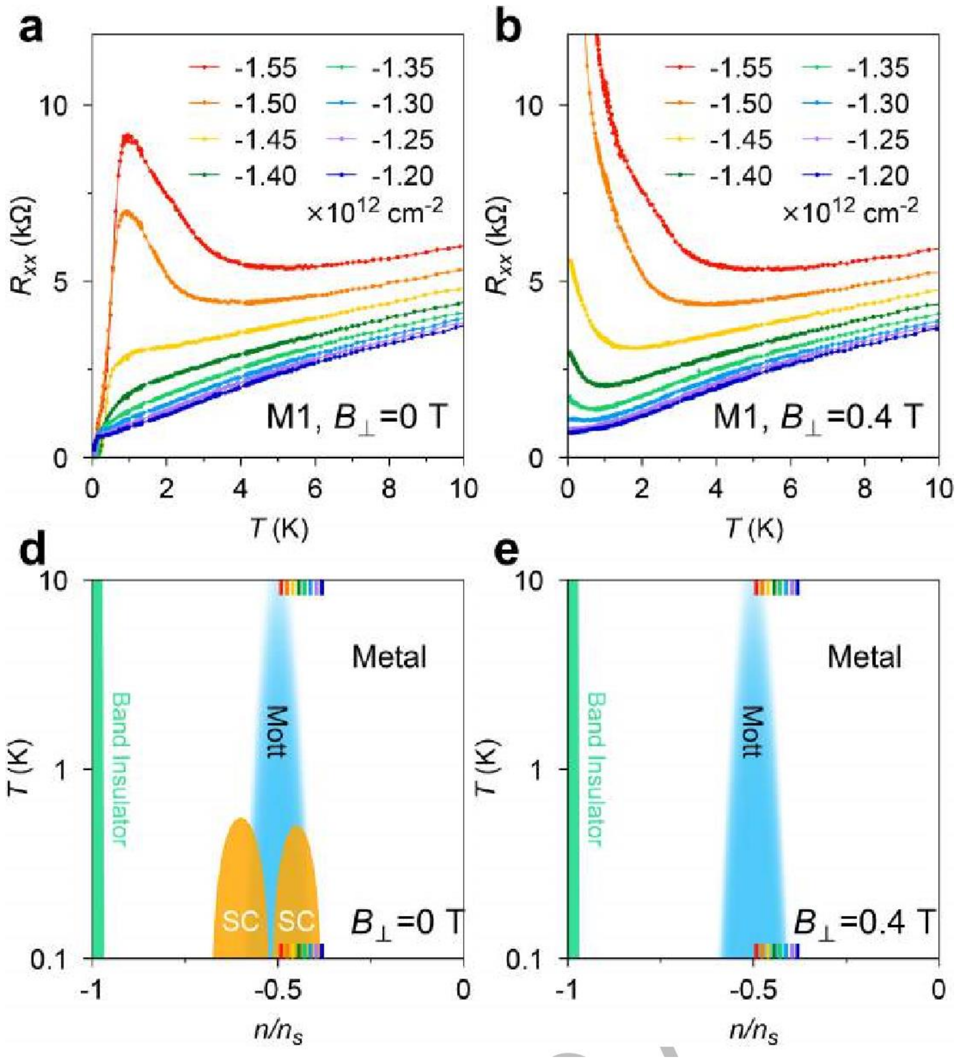

Resistivity changing from metallic to insulating and finally to SC behavior is consistent with intertwined SC and density wave instabilities .

In-plane upper critical fiend is close to Pauli limit, indicates spin-singlet pairing

If so, our theory proposes “Mott” insulator is a CDW that breaks translation & preserves spin rotation

Open Questions

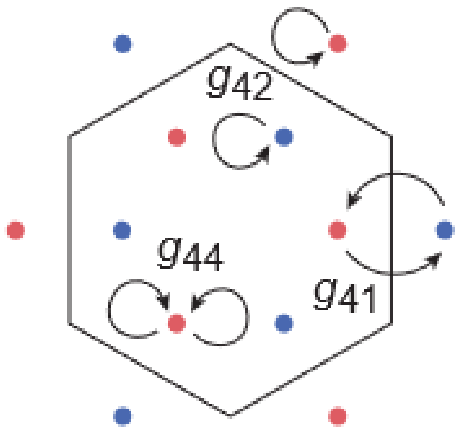

Intertwinement of spin-singlet SC and CDW requires repulsive intervalley density interaction and attractive intervalley exchange interaction at the cutoff energy scale of patch theory.

Possbible origin of attraction: mediated by intervalley electron-phonon coupling ?

negative Hund-coupling? (c.f. Kivelson et al)

Strong coupling description of CDW insulator ?

Experimental signature of CDW: STM ?